Composite Organization of the Cobalamin Binding and Cubilin Recognition Sites of Intrinsic Factor†

Sergey N. Fedosov,*,‡ Natalya U. Fedosova,§ Lars Berglund,|| Søren K. Moestrup,⊥ Ebba Nexø,@ and Torben E. Petersen‡

Protein Chemistry Laboratory, Department of Molecular and Structural Biology, University of Aarhus, Science Park, Gustav Wieds Vej 10, 8000 Aarhus C, Denmark, Department of Biophysics, University of Aarhus, Ole Worms Alle 185, 8000 Aarhus C, Denmark, Cobento Biotech A/S, Science Park, Gustav Wieds Vej 10, 8000 Aarhus C, Denmark, Department of Medical Biochemistry, University of Aarhus, Ole Worms Alle 170, 8000 Aarhus C, Denmark, and Department of Clinical Biochemistry, AS Aarhus University Hospital, Nørrebrogade 44, 8000 Aarhus C, Denmark

Received September 23, 2004; Revised Manuscript Received December 9, 2004

ABSTRACT: Intrinsic factor (IF_{50}) is a cobalamin (Cbl)-transporting protein of 50 kDa, which can be cleaved into two fragments: the 30 kDa N-terminal peptide IF_{30} and the 20 kDa C-terminal glycopeptide IF_{20}. Experiments on binding of Cbl to IF_{30}, IF_{20}, and IF_{50} revealed comparable association rate constants ($k_{+Cbl} = 4 \times 10^6$, 14×10^6, and 26×10^6 M^{-1} s^{-1}, respectively), but the equilibrium dissociation constants were essentially different ($K_{Cbl} = 200$ μM, 0.2 μM, and ≤ 1 pM, respectively). The smaller fragment, IF_{20}, had unexpectedly high affinity for Cbl; however, efficient retention of the ligand required the presence of both fragments. Detailed schemes of the interaction of Cbl with IF_{50} and with IF_{30} and IF_{20} are presented, where the sequential attachment of Cbl to the IF_{20} and IF_{30} domains plays the key role in recognition and retention of the ligand. Each isolated fragment of IF was tested for the binding to the specific receptor cubilin in the presence or absence of Cbl. Neither apo nor holo forms of IF_{20} and IF_{30} were recognized by the receptor. When two fragments were mixed and incubated with Cbl, they associated into a stable complex, IF_{30+20}·Cbl, which bound to cubilin as well as the noncleaved IF_{50}·Cbl complex. We suggest that formation of the cubilin recognition site on IF is caused by assembly of two distant domains, which allows the saturated protein to be recognized by the receptor. The obtained parameters for ligand and receptor binding indicate that both full-length IF_{50} and the fragments may be involved in Cbl assimilation.

Intrinsic factor (IF)[1] is one of three cobalamin (Cbl or vitamin B_{12})-transporting proteins present in a mammalian organism (*1*−*3*). Abundant secretion of IF into the intestinal tract is necessary for normal assimilation of the vitamin. IF is relatively resistant to proteolysis, and its binding activity exceeds by far the amount of Cbl liberated from food (*1*, *3*). High selectivity toward Cbl (*4*) and high affinity of the saturated protein for the specific receptor (*5*, *6*) distinguish IF from other Cbl transporters. The above features guarantee (i) uptake of the physiologically active ligand and (ii) accessibility of the receptor, which is not blocked by an excess of unsaturated IF.

IF is employed as an additive to many vitamin preparations as well as in the Schilling test. The binder is also used for measurement of Cbl levels in biological samples (*7*, *8*). Therefore, understanding the mechanisms behind IF action is important for proper application of this protein for both analytical and medical purposes. The continuing controversy over the affinity of specific binders for Cbl with exceptional dispersion of the results [$K_{Cbl} = 10^{-14}$−10^{-8} M (*9*−*12*)] emphasizes the significance and necessity of the thorough kinetic analysis.

In our previous work (*13*), we investigated oligomerization of the full-length protein IF_{50} and its two proteolytic fragments upon Cbl binding. The first fragment, IF_{30}, represented the N-terminal peptide of 30 kDa with most of the conservative residues and all disulfide bridges. The second fragment, IF_{20}, contained only 13 kDa of the C-terminal sequence, and the rest of its mass ($\approx$7 kDa) originated from the attached carbohydrates. Dissection of IF provided an excellent opportunity to gain deeper insight into the role of different domains during ligand binding and receptor recognition. A two-domain organization of IF was suggested, where assembly of the distant units, IF_{30} and IF_{20}, appeared to be important for adjustment of the ligand inside the binding site. The two domains mentioned above were connected by a link, which seemed to be responsible for dimerization of the full-length protein after its saturation with Cbl. Dimers were, however, unstable under in vitro conditions.

In this paper, we quantify (i) binding of Cbl to IF and its fragments, (ii) assembly of the IF domains in the presence

† This work was supported by the Eureka program (CT-T2006), Cobento Biotech A/S, and the Lundbeck Foundation.

* To whom correspondence should be addressed. Telephone: (+45) 89 42 50 92. Fax: (+45) 86 13 65 97. E-mail: snf@imsb.au.dk.

‡ Department of Molecular and Structural Biology, University of Aarhus.

§ Department of Biophysics, University of Aarhus.

|| Cobento Biotech A/S.

⊥ Department of Medical Biochemistry, University of Aarhus.

@ AS Aarhus University Hospital.

[1] Abbreviations: AP, active protein coefficient; B_{12}, vitamin B_{12}; Cbl, cobalamin (H_2OCbl, aquocobalamin if not stated otherwise); CNCbl, cyanocobalamin; ^{57}Cbl, radioactive ligand [^{57}Co]CNCbl; Gd-nHCl, guanidine hydrochloride; IF, intrinsic factor; P_i buffer, NaH_2PO_4/Na_2HPO_4 buffer.

10.1021/bi047936v CCC: $30.25
Published on Web 02/10/2005

of Cbl, and (iii) interaction of the IF variants with cubilin. A composite organization of both the Cbl binding and receptor recognition sites is suggested.

EXPERIMENTAL PROCEDURES

Materials

All standard chemicals were purchased from Merck, Roche Molecular Biochemicals, and Sigma-Aldrich. H_2OCbl/CNCbl and [^{57}Co]CNCbl were obtained from Sigma-Aldrich and ICN Pharmaceutical Ltd., respectively. The H_2OCbl specific matrix CobaPure was a product of Cobento Biotech A/S.

Methods

Expression and Purification of Human IF. The recombinant IF was produced from plants as described in our previous publications (*6*, *13*). IF from gastric juice was purified according to the method of ref *14*.

Spectral Measurements and Molar Absorbance. The molar absorbancies of apo-IF and its fragments were calculated from the known number of Trp, Tyr, and Cys-Cys residues according to the equation $\epsilon_{280} = 5500N_{Trp} + 1490N_{Tyr} + 125N_{S-S}$ M^{-1} cm^{-1} (*15*). The molar absorbance of unsaturated IF at 354 nm was calculated from the relation $\epsilon_{354} = \epsilon_{280}(A_{354}/A_{280})$.

The specific adsorption ($\Delta\epsilon$) of the protein-associated ligand was measured in the following way. Subsaturating concentrations of Cbl (5 μM) were added to IF_{50} (25−35 μM), and the change in the optical response ΔA at 280 and 354 nm was related to the concentration of added Cbl. Increments ($\Delta\epsilon$) to the original molar absorbance of apo-IF (ϵ_0) were calculated. The molar absorbance of 100% saturated (100% pure) holo-IF corresponded to the relation $\epsilon = \epsilon_0 + \Delta\epsilon$. These coefficients were used to calculate the faction of active protein in the obtained preparations; see the next paragraph and section 1 of the Appendix.

Saturation of IF and Removal of Free H_2OCbl. Saturated proteins IF_{50}·Cbl and IF_{30+20}·Cbl (10−30 μM, 0.2 M P_i, pH 7.5) were produced by adding a 30−50% molar excess of H_2OCbl. Free H_2OCbl was removed via adsorption for 10 min on the specific matrix CobaPure (15−20% of the sample volume).

Stopped-Flow Experiments on Cbl Binding. Attachment of H_2OCbl to IF_{50}, IF_{30}, IF_{20}, or a protein−protein model was monitored on a DX.17MV stopped-flow spectrofluorometer (Applied Photophysics) in 0.2 M P_i at pH 7.5 and 20 °C. Cbl served as a reporting agent because of the changing absorbance of the γ-peak caused by protein binding (*11*, *16*). The optical response was recorded at A_{355} with a band-pass of 18.6 nm. When it was possible, we used constant Cbl and variable protein concentrations to maintain the minimal absorbance of the sample.

Dissociation of the Peptide−Ligand Complexes. The stability of the peptide−ligand complexes was investigated in an assay where IF_{30} or IF_{20} competed with the specific resin CobaPure for H_2OCbl. This novel material from Cobento Biotech is capable of H_2OCbl binding ($k_{+ads} = 20$ M^{-1} s^{-1}, $k_{-ads} = 10^{-4}$ s^{-1}, $K_d \approx 5$ μM) at 20 °C and pH 3−7. A concentration of the active groups in the matrix of 6 mM ensured efficient H_2OCbl binding even in the diluted suspension. The peptide−ligand sample (300 μL) was mixed with the resin suspension (10 μL, 1:1 matrix:water ratio), and the final concentrations of the reagents were as follows: 20 μM IF, 15 μM Cbl, and ≈100 μM CobaPure active groups. The sample was incubated with mild agitation in 0.2 M P_i at pH 7.5 and 20 °C. After different time intervals, the suspension was briefly centrifuged (for 10 s at 14 000 rpm), whereupon the concentration of Cbl in the supernatant was measured spectroscopically. The supernatant and the pellet were mixed again, and incubation was continued. The time of the reaction included only the suspended state of the sample. In the alternative filtration setup, 1−2 mL of the IF/Cbl/resin suspension was prepared, and 200 μL fractions were quickly filtered at time intervals. The absorbance in the filtrate was then measured. Filtration and centrifugation methods gave similar results.

Cbl Exchange in the Firm IF·Cbl Complexes. Dissociation of the IF_{30+20}·H_2OCbl or IF_{50}·H_2OCbl complex (each at 12 μM in 0.2 M P_i at pH 7.5 and 20 °C) was initiated by mixing the sample with 50 μM CNCbl as described previously (*11*). The transition from the IF·H_2OCbl complex to the IF·CNCbl complex was monitored at A_{361} and A_{352} values determined after adsorption of free Cbls on charcoal. The total change in absorbance ($\Delta A_{361} + \Delta A_{352} = 0.3-0.4$) during the reaction time of 16 h was sufficient to make the measurements reliable. Calculation of the relative change in absorbance (A_{361}/A_{352}) eliminated any possible error introduced by partial protein precipitation.

Binding of [^{57}Co]CNCbl to IF at Low Protein Concentrations. The experiments were performed by a modified charcoal method (*17*). In short, a preparation of unsaturated IF_{50} or IF_{30} and IF_{20} (80−100 pM) was mixed with ^{57}Cbl at concentrations varying from 5 to 230 pM. The samples were incubated for 10 min (20 °C) or 20 h (5 °C), whereupon the excess of the free ligand was adsorbed on charcoal for 10 min. The protein-associated radioactivity was measured in the supernatant. Radioactivity in the control samples (without IF) was subtracted from that in the experimental samples (with IF).

Binding of Cbl at Physiological Concentrations. The assay was carried out as described in the previous paragraph with certain modifications. The protein was taken in high excess (10−50 nM IF_{50} or IF_{30} with IF_{20}) and mixed with ^{57}Cbl (2 nM). The sample of IF_{30} and IF_{20} (slow Cbl binding) could contain a small contamination of IF_{50} (fast Cbl binding). Therefore, a control experiment was carried out, in which the potential binding activity of IF_{50} was suppressed by "cold" Cbl (2 nM) prior to the binding of the "hot" Cbl. No difference between the two setups was found. Small portions of the reaction medium were mixed with charcoal at time intervals. When the reaction proceeded (20 min), all the samples were incubated with charcoal for an additional 10 min and centrifuged. Radioactivity was measured in the supernatant.

Binding of IF to the Receptor. Binding of IF to immobilized cubilin was performed on a BIAcore 2000 instrument as described previously (*5*, *6*, *13*).

Kinetic Analysis. Fitting was performed with help of KyPlot 4 (Kyence Inc.) and Gepasi 3.2 (*18*). The statistical data are presented as the mean ± the standard deviation.

RESULTS

Spectral Characteristics of the Unsaturated IF. Isolation of the full-length protein, IF_{50}, and fragments IF_{30} and IF_{20}

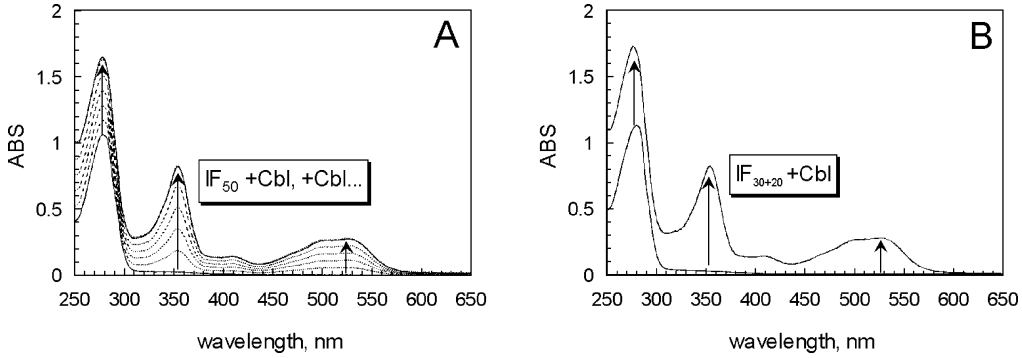

FIGURE 1: Absorbance spectra of the native and cleaved forms of IF. The data were obtained in 0.2 M P_i buffer at pH 7.5 and 20 °C. The amplitudes of optical change at 280 and 355 nm upon addition of H_2OCbl were used to calculate $\Delta\epsilon$ in Table 1. (A) Absorbance spectra of full-length IF_{50}. The bottom solid line is the spectrum for 26 μM apo-IF_{50} devoid of Cbl. The dashed spectra were obtained after addition of 5 × 5.0 μM Cbl (the amplitudes were corrected for dilution). The top solid line is the spectrum of the completely resaturated protein. (B) Absorbance spectra of the cleaved protein, IF_{30}+IF_{20}. The bottom spectrum was recorded for a mixture of 26 μM IF_{20} and 30 μM IF_{30}. The top spectrum is for the same protein resaturated with Cbl.

Table 1: Coefficients of Molar Absorbance (M^{-1} cm^{-1}) for IF and the IF·H_2OCbl Complex at pH 7.5

IF form	280 nm	354 nm
apo-IF_{30}, ϵ_0	22 900	500
apo-IF_{20}, ϵ_0	19 100	2000
apo-IF_{50}, ϵ_0	42 000	2500
H_2OCbl	19 900	23200[a]
IF_{50}·H_2OCbl, $\Delta\epsilon$	20 600	31000
IF_{50}·H_2OCbl (100%)	62 600[b]	33500[b]

[a] The data for ϵ_{352} from ref 11. [b] Molar absorbance of an absolute preparation (100% pure and 100% active). All coefficients were determined with a standard deviation 1−3% from the mean value (n = 15).

was described in our previous publication (*13*). All protein samples were devoid of Cbl and renatured prior to the binding experiments (*13*). Absorbance spectra of the apo forms of IF_{50} and IF_{30} with IF_{20} are shown in Figure 1 (bottom curves). The coefficients of molar absorbance were calculated as described in Materials and Methods and are presented in Table 1.

Absorbance Ratio of the Active Protein. The optical response from H_2OCbl was measured at the subsaturating concentrations of the ligand (Figure 1A). This allowed us to establish the increments $\Delta\epsilon$ of the Cbl molar absorbance added to that of the apoprotein (ϵ_0, Table 1). The parameters ϵ_0, $\Delta\epsilon$, and R (A_{280}/A_{354}) were used to calculate the fraction of the active protein (AP) as discussed in section 1 of the Appendix. Estimated values of AP were 0.97 ± 0.03 for IF_{50} and >0.85 for IF_{30} with IF_{20}. Absorbance spectra of the saturated IF_{50}·Cbl and IF_{30+20}·Cbl complexes did not differ from each other (Figure 1A,B) and from that of the protein, which was not subjected to GdnHCl treatment (*6*).

As follows from Table 1 and our previously published data (*11*, *16*, *19*), the spectrum of Cbl is sensitive to the surrounding conditions. Therefore, the change in intensity of the γ-peak during the binding experiments was related to the binding of Cbl to IF and the following protein association.

Binding of Cbl to the N-Terminal Fragment, IF_{30}. H_2OCbl at a constant concentration was exposed to varying concentrations of the IF_{30} peptide, and the optical response was followed over time (Figure 2A). The recorded reaction corresponded to the reversible binding (see section 2 of the Appendix). Extrapolation to the infinite concentration of IF_{30} according to the hyperbolic function or eq 2.1 gave the maximal amplitude equal to 0.054 ± 0.003 or 0.047 ± 0.003 cm^{-1}, respectively. On that basis, the coefficient of relative optical response was calculated (ϵ_Δ = 2500 ± 500 M^{-1} cm^{-1}), whereupon the ϵ_Δ values of 2000, 2500, and 3000 M^{-1} cm^{-1} were sequentially assigned as the constants in eq 2.2. Three curves were fitted using the same ϵ_Δ, and for each ϵ_Δ, the optimal rate constants were calculated by regression analysis: k_{30+Cbl} = (3.0 ± 0.2) × 10^6, (3.4 ± 0.3) × 10^6, and (4.1 ± 0.5) × 10^6 M^{-1} s^{-1} and k_{30-Cbl} = 100 ± 20, 140 ± 10, and 180 ± 20 s^{-1}, respectively. The final values are listed in Table 2 with maximal dispersion of the results obtained. This experiment allowed us to make an estimate of the dissociation constant $K_{30,Cbl}$ (40 ± 20 μM); i.e., the affinity of IF_{30} for Cbl was low, yet detectable.

Binding of Cbl to the C-Terminal Fragment, IF_{20}. The analogous experiment with the glycopeptide IF_{20} demonstrated significantly higher affinity for the ligand (Figure 2B). The data that are presented suggest that 20 μM Cbl could already saturate this fragment. Therefore, the final fit was carried out according to the irreversible model (eq 2.4) with two regression coefficients: ϵ_Δ = 1200 ± 100 M^{-1} cm^{-1} and k_{20+Cbl} = (14 ± 3) × 10^6 M^{-1} s^{-1} (n = 3).

Association of IF_{30} and IF_{20}·Cbl. Injection of IF_{30} into the preincubated IF_{20}·Cbl sample caused increase in absorbance at 355 nm (Figure 2C). The effect was ascribed to association of the peptides, because the observed velocity was dependent on the IF_{30} concentration. The fitting was performed according to eq 2.4 for the irreversible binding with an ϵ_Δ of 3400 ± 200 M^{-1} cm^{-1} and a k_{+30} of (4 ± 0.5) × 10^6 M^{-1} s^{-1} (n = 3).

Binding of Cbl to the Full-Length Form, IF_{50}. Addition of Cbl to the full-length protein induced a biphasic response (Figure 2D). The first phase had a higher amplitude, was Cbl-dependent, and seemed to represent attachment of Cbl to IF_{50}. The second phase was Cbl insensitive, and its expression varied between IF_{50} preparations from 20 to 50% of the total amplitude (ΔA = 0.05 ± 0.005 cm^{-1}). Since the purity of the protein, its molecular mass (*13*), equilibrium binding of Cbl, and receptor recognition were similar and comparable to those of gastric IF (this publication and ref *13*), each IF_{50} preparation was considered to be uniform. Therefore, variations in the second phase were ascribed to some conformational differences in IF apo forms, possibly, originating from the denaturing−renaturing procedure. This

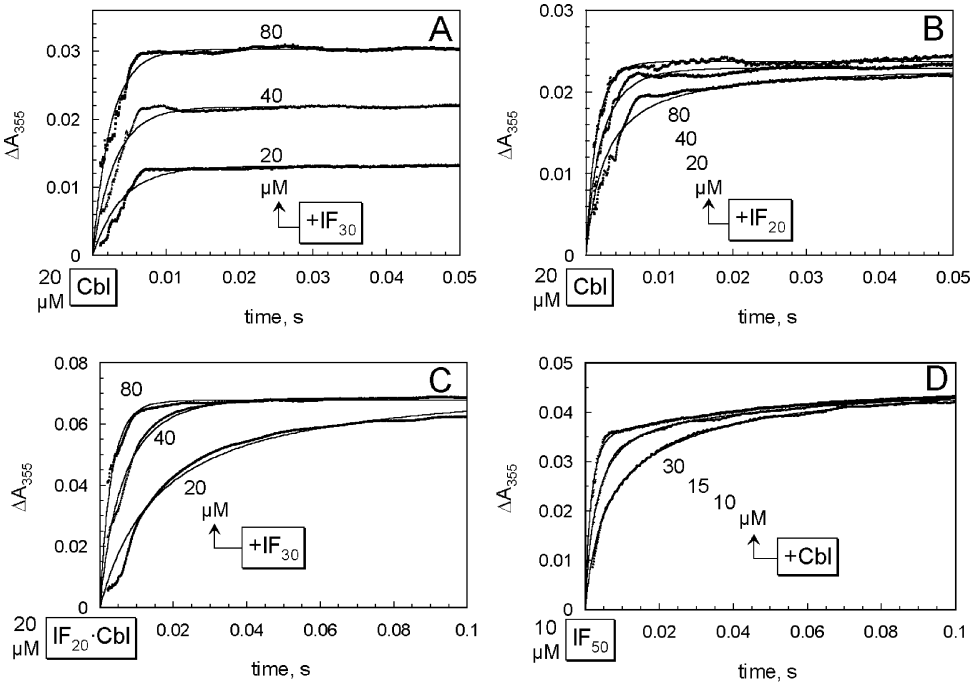

FIGURE 2: Stopped-flow measurements of the absorbance changes induced by H_2OCbl binding. All reactions were performed in 0.2 M P_i buffer at pH 7.5 and 20 °C, and the change in absorbance at 355 nm was recorded. Final concentrations of the binding species in the detection cell are given. The calculated rate constants are presented in Table 2. See the main text for the details. (A) Binding of Cbl (20 μM) to IF_{30} (20, 40, and 80 μM). The data were fitted using eq 2.2. (B) Binding of Cbl (20 μM) to IF_{20} (20, 40, and 80 μM). The data were fitted using eqs 2.2 and 2.4. (C) Binding of IF_{20}·Cbl (20 μM) to IF_{30} (20, 40, and 80 μM). The data were fitted using eq 2.4. (D) Binding of Cbl (10, 15, and 30 μM) to IF_{50} (10 μM). The data were fitted according to a two-step model (section 3 of the Appendix).

Table 2: Rate Constants of Cbl Binding and IF Oligomerization

reaction	k_+ ($\times 10^{-6}$ M^{-1} s^{-1})	k_- (s^{-1})	K_{diss}
$IF_{30} + Cbl \leftrightarrow IF_{30}$·Cbl	$k_{30+Cbl} = 3.5 \pm 0.6^a$	$k_{30-Cbl} = 140 \pm 40^a$	$K_{30,Cbl} = 40 \pm 20$ μM^a $= 200 \pm 80$ μM^b
$IF_{20} + Cbl \leftrightarrow IF_{20}$·Cbl	$k_{20+Cbl} = 14 \pm 3^a$	$k_{20-Cbl} = 4 \pm 3^{a,b}$	$K_{20,Cbl} = 0.2 \pm 0.2$ μM^b
$IF_{30} + IF_{20}$·Cbl $\leftrightarrow IF_{30+20}$·Cbl	$k_{+30} = 4.0 \pm 0.5^a$	$k_{-30} = (2.7 \pm 0.2) \times 10^{-5\,c}$	$K_{30} = 7 \pm 1$ $pM^{a,c}$
$IF_{20} + IF_{30} + Cbl \leftrightarrow IF_{30+20}$·Cbl		real equilibrium, $K_{eq} = K_{20,Cbl}K_{30} = 2 \times 10^{-18}$ M^2	
$IF_{20} + Cbl \leftrightarrow IF_{30+20}$·Cbl		apparent equilibrium, $K_{3020,Cbl} = (K_{20,Cbl}K_{30})/[IF_{30}]$ (M)	
$IF_{50} + Cbl \leftrightarrow IF_{50}\cdots Cbl$ (1)	$k_{50+1} = 26 \pm 3^a$ $= 60 \pm 2^c$ (A) $= 40 \pm 4^c$ (B)	$k_{50-1} \leq 4^{a,c}$	$K_{50,1} \leq 0.1$ $\mu M^{a,c}$
$IF_{50}\cdots Cbl \leftrightarrow IF_{50}$·Cbl (2)	$k_{50+2} = 20 \pm 5$ $s^{-1\,a}$	$k_{50-2} \leq 10^{-4\,a,c}$	$K_{50,2} \leq 10^{-5\,a,c}$
$IF_{50} + Cbl \leftrightarrow IF_{50}$·Cbl		equilibrium, $K_{50,Cbl} = K_{50,1}K_{50,2} \leq 10^{-12}$ M^c (A) $= (3 \pm 1) \times 10^{-12}$ M^c (B)	
$2IF_{50}$·Cbl $\leftrightarrow (IF_{50}$·$Cbl)_2$	$>0.01^d$	$>0.01^d$	1 ± 0.1 μM^d

[a] Determined from the data in Figure 2. [b] Determined from the data in Figure 3. [c] Determined from the data in Figure 4. [d] From ref *13*. The values are presented as the mean ± the standard deviation.

subject requires a separate survey, which is now in progress. For the binding kinetics aimed for this publication, the curves in Figure 2D were simulated according to the two-step model: (i) Cbl binding for which $\Delta A_1 = 0.035 \pm 0.001$ cm^{-1} and $k_{50+1} = (26 \pm 3) \times 10^6$ M^{-1} s^{-1} and (ii) conformational transition for which $\Delta A_2 = 0.01 \pm 0.001$ cm^{-1} and $k_{50+2} = 20 \pm 5$ s^{-1} (see section 3 of the Appendix for the details).

Dissociation of Cbl from the IF Fragments. In the previous paragraphs, we analyzed the binding of Cbl to the fragments (Figure 2A,B) and estimated their k_{+Cbl} and k_{-Cbl}. Yet, the precision of measurements could be questioned. Therefore, the affinity of the fragments for Cbl was probed directly in a competition assay employing an insoluble Cbl-specific adsorbent CobaPure (Figure 3). The preliminary experiment showed that the resin efficiently removed free Cbl from the water phase so that its concentration decreased in a few minutes from 15 to 0.3 ± 0.05 μM (Figure 3A, bottom curve). The presence of IF_{30} in the solution did not essentially decelerate Cbl absorption [Figure 3A (△)], whereas added IF_{20} forced the process to slow [Figure 3A (□)]. It was concluded that the small fragment, IF_{20}, had a higher affinity for Cbl than IF_{30}. However, the most noticeable effect was observed for the IF_{30}/IF_{20}/Cbl and IF_{50}/Cbl mixtures, when no visible removal of the ligand from the water phase was detected (Figure 3A, top curves).

The preliminary experiment (Figure 3A) showed that the velocity v_{ads} of Cbl adsorption on the resin was essentially slower than the velocity of equilibration of Cbl with the IF fragments (Figure 2A,B). In addition, the CobaPure−Cbl interaction was hampered by IF due to the fast IF + Cbl ↔ IF·Cbl equilibrium, where the IF·Cbl complex seemed to be much less reactive with the resin than free Cbl. This made

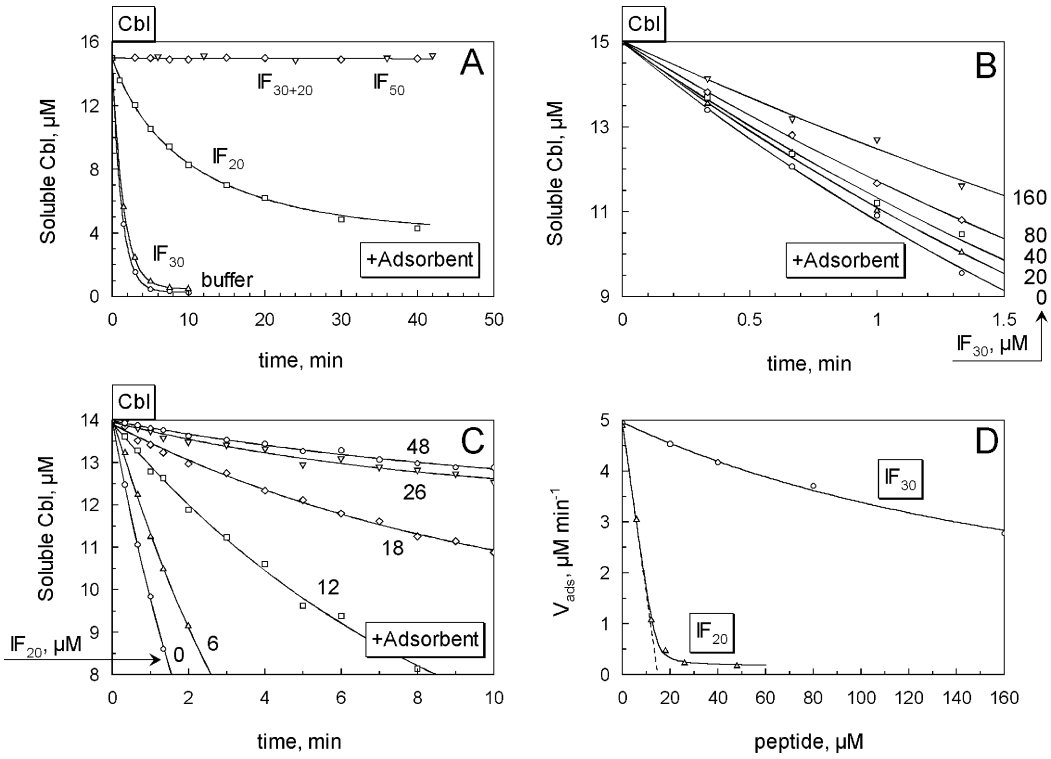

FIGURE 3: Suppression of H_2OCbl adsorption on the CobaPure resin by IF variants. All reactions were performed in 0.2 M P_i buffer at pH 7.5 and 20 °C. Precipitation of Cbl was started by mixing the sample (Cbl with or without IF) with the insoluble Cbl-adsorbent CobaPure (see Materials and Methods). The decreasing level of Cbl in the solution was followed over time. The theoretical background is discussed in section 4 of the Appendix. The calculated constants are presented in Table 2. (A) Qualitative effect of different IF forms. The reaction was conducted at the following initial concentrations: 15 μM Cbl, 20 μM IF, and ≈250 μM active groups of the resin. (B) Quantitative effect of IF_{30}. The reaction was conducted at the following initial concentrations: 15 μM Cbl, 0−80 μM IF_{30}, and ≈100 μM active groups of the resin. (C) Quantitative effect of IF_{20}. The reaction was conducted at the following initial concentrations: 14 μM Cbl, 0−48 μM IF_{20}, and ≈100 μM active groups of the resin. (D) Initial velocity of Cbl precipitation as a function of the peptide concentration. The curves were fitted using eq 4. The calculated dissociation constants K_{20Cbl} and K_{30Cbl} of the corresponding peptide−Cbl complexes are given in Table 2. The dashed line is a tangent at 0 M IF, and its intersection with the [IF] axis is equal to $[IF_{20}] + K_{20Cbl}$.

it possible to estimate the IF·Cbl dissociation constant. In the simplest case, adsorption of Cbl in time could be approximated by an exponent with $k = k_{+ads}/(1 + IF/K_{IFCbl})$, yet, comparable concentrations of the reagents and the additional very slow interaction of IF·Cbl with the resin required a more elaborate analysis (section 4 of the Appendix).

To determine the dissociation constants of the peptide·Cbl complexes, we varied concentrations of IF_{30} and IF_{20} and calculated the corresponding initial velocities of Cbl adsorption, v_{ads}, from the differentiated exponential approximations (solid lines in Figure 3B,C). Dependencies of v_{ads} on IF_{30} and IF_{20} (Figure 3D) were fitted using eq 4 which gave the dissociation constants of the fragment−Cbl complexes: $K_{30,Cbl} = 200 \pm 80$ μM and $K_{20,Cbl} = 0.2 \pm 0.2$ μM, respectively. The following velocities of adsorption were calculated as $[IF_{20}]$ or $[IF_{30}] \rightarrow \infty$: $v_{20,es} = 0.2 \pm 0.1$ and $v_{30,es} = 0 \pm 1$ μM min^{-1}, respectively. This points to slow interaction of the IF_{20}·Cbl complex with the matrix.

The strong binders IF_{50} and IF_{30} with IF_{20} completely protected Cbl from adsorption on the resin, and the method described above could not be used for determination of their affinities for Cbl.

Saturation of IF with Radioactive ^{57}Cbl at Low Protein Concentrations. The full-length recombinant binder IF_{50} and the equimolar mixture of IF_{30} and IF_{20} (all diluted to 80−90 pM) were subjected to saturation with increasing concentrations of the radioactive ligand [^{57}Co]CNCbl (95 ± 2 cpm/pM); see Figure 4A. The incubation time of 10 min was clearly not sufficient for the reaction to reach the equilibrium, when comparing the 10 min and 20 h curves. This was particularly visible at the point of equivalence ($IF_{50} \approx {}^{57}$Cbl) where the reaction decelerated progressively in accordance with the product of concentrations ($v = k_{+Cbl}[IF][{}^{57}Cbl]$). As a consequence, the transient 10 min curve could not be fit according to the equilibrium equation (Appendix, eq 2.1). On the other hand, a time-dependent function (eq 2.4) with a constant t of 10 min and a variable S_0 (^{57}Cbl) seemed to be a fair approximation for the 10 min data. The fitting was performed with the assigned constant $\epsilon_\Delta = 95$ cpm/pM and two regression parameters: $[IF_{50}] = 83 \pm 1$ pM and $k_{+Cbl} = (60 \pm 2) \times 10^6$ M^{-1} s^{-1}. The rate constant of Cbl attachment was somewhat higher than that in the stopped-flow measurements (Figure 2D).

In the "near equilibrium experiment" for IF_{50} and IF_{30} with IF_{20} in Figure 4A, the incubation was conducted for 20 h, and the produced curves were fit according to the reversible mechanism (eq 2.1). The following results were obtained: $[IF_{50}] = 90 \pm 1$ pM, $K_{50,Cbl} = 0.1 \pm 0.1$ pM, and $[IF_{30}+IF_{20}] \approx 90$ pM, and $K_{3020,Cbl} \approx 2$ nM. Both dissociation constants were not precise because of either very high or very low affinity for the ligand under the conditions used in the experiment. Therefore, we confine us to the statement that $K_{50,Cbl} < 1$ pM and $K_{3020,Cbl} > 1$ nM. The second coefficient $K_{3020,Cbl}$ was actually not a constant because it is expected to be dependent on IF_{30} concentration ($K_{3020,Cbl} = K_{eq}/[IF_{30}]$

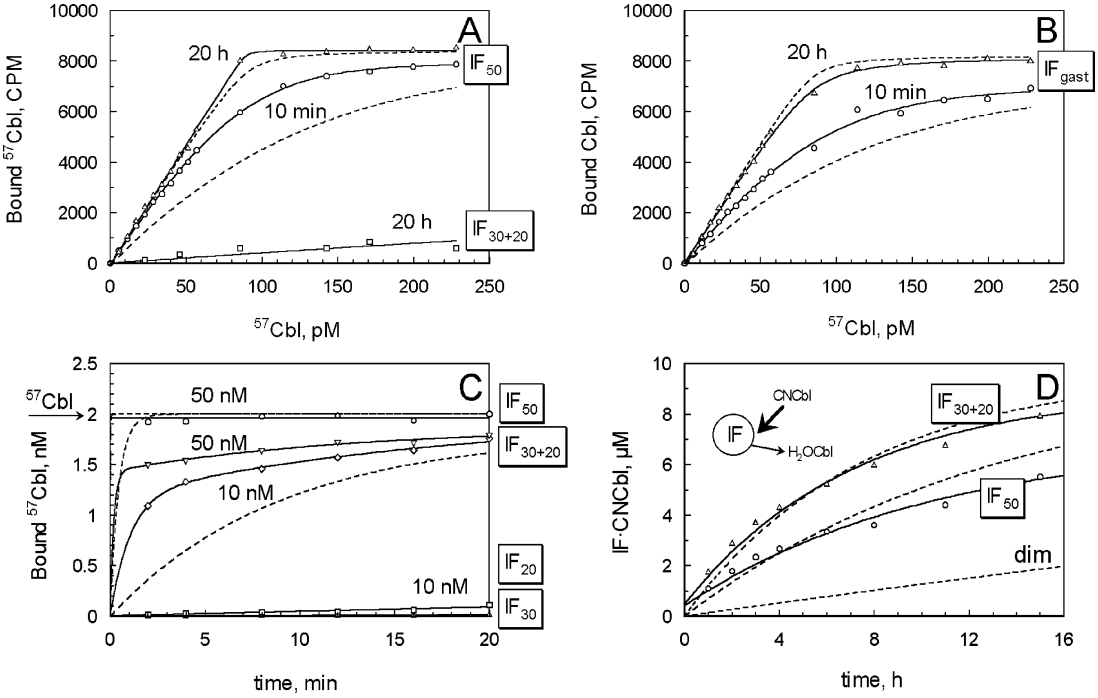

FIGURE 4: Interaction between [^{57}Co]CNCbl and IF at different protein concentrations. (A) Saturation of recombinant IF at a low protein concentration (≈85 pM). IF_{50} or the equimolar mixture of IF_{30} and IF_{20} was incubated with different concentrations of ^{57}Cbl for either 10 min or 20 h. Protein-associated radioactivity (95 ± 2 cpm/pM) was measured by a charcoal method. The fit of the 10 min transition curve and the 20 h near-equilibrium data was performed on the basis of eqs 2.4 and 2.1, respectively (solid lines). The results are presented in Table 2. Dashed curves in all panels demonstrate theoretical simulations performed on the basis of the final model; see the text for the details. (B) Saturation of gastric IF at a low protein concentration (≈80 pM). All data are as in panel A. (C) Binding of ^{57}Cbl to recombinant IF at physiological concentrations. ^{57}Cbl (2 nM) was incubated with 10−50 nM IF, and the appearance of the stable protein−^{57}Cbl complexes was followed over time by a charcoal method. (D) Cbl exchange at high protein concentrations. The IF_{50}·H_2OCbl or IF_{30+20}·H_2OCbl complex (12 μM) was mixed with CNCbl (50 μM), and displacement of the endogenous ligand by the exogenous one was followed over time by absorbance measurements.

$= [IF_{20}][Cbl]/[IF_{30+20}Cbl])$.

The analogous test was performed with gastric IF. The analysis gave the following values: $IF_{gast} = 74 \pm 2$ pM and $k_{+Cbl} = (40 \pm 4) \times 10^6$ M^{-1} s^{-1} for the 10 min curve and $IF_{gast} = 86 \pm 1$ pM and $K_{gIF,Cbl} = 3 \pm 1$ pM for the near-equilibrium 20 h experiment.

Binding of Cbl to IF at Physiological Concentrations. Interaction between [^{57}Co]CNCbl and different variants of recombinant IF was followed over time at physiological concentrations: 2 nM ^{57}Cbl and 10−50 nM IF. As expected, the IF_{50} + Cbl reaction was already finished after incubation for 2 min (the 50 nM curve is shown in Figure 4C). An equimolar mixture of the IF_{30} and IF_{20} fragments (10−50 nM) was also quite efficient, and the binding reaction was generally accomplished after incubation for 10 min (Figure 4C, the middle curves). On the other hand, neither IF_{30} nor IF_{20} could bind Cbl when taken separately (the curves for 10 nM peptides are shown in Figure 4C). An attempt to interpret the biphasic kinetics of the IF_{30}−IF_{20}−Cbl binding in Figure 4C is made in the Discussion.

Dissociation of IF·Cbl Complexes at High Concentrations. Detachment of H_2OCbl from the binder was initiated by a 4-fold excess of CNCbl in the medium. The data in Figure 4D were fitted using an exponent (solid line) whereupon the initial velocity of the process was calculated by differentiation of the approximating function. It was equal to $v_{0,Cbl} = k_{-app}[IF{\cdot}H_2OCbl]$ and was independent of the mechanism; however, the interpretation of k_{-app} essentially depended on the chosen model. At present, we simply report the following values: $k_{-app} = 0.10 \pm 0.01$ and 0.05 ± 0.01 h^{-1} for IF_{30+20}·Cbl and IF_{50}·Cbl, respectively. Interestingly enough, the velocity of the ligand exchange for the GdnHCl-treated protein was 2-fold slower than that of the preparation without GdnHCl treatment (*13*).

Simulation of Cbl Binding. The deduction of the final kinetic scheme for Cbl binding to IF is presented in the Discussion. Most of the rate constants were obtained from the experiments with results depicted in Figures 2 and 3. Therefore, the behavior of the model was verified using the data of another test (Figure 4), which was conducted by another method and under different conditions. The theoretical curves (Figure 4, dashed lines) were generated with help of the simulating program Gepasi (*18*) and the suggested schemes. The model showed a reasonable agreement with the experimental data, yet a better correspondence could be obtained by increasing k_{+Cbl} from 2×10^7 to 5×10^7 M^{-1} s^{-1} (not shown). A possible explanation of the deviation visible in Figure 4C is given in the Discussion.

Binding of IF Variants to Cubilin. BIACore analysis of interaction with the specific receptor showed no binding of IF_{50} and Cbl when they were added separately to the cubilin-coated chip (Figure 5A). Mixing of IF_{50} and Cbl prior to the receptor binding initiated a response from the chip (Figure 5A). The recorded curves were similar to those observed for the original protein, which was not exposed to GdnHCl (*13*).

The analogous experiment was performed with the separated fragments. The binding was observed for neither IF_{30} nor IF_{20} with or without Cbl (Figure 5B,C). A slight response in Figure 5B was caused by artificial adsorption of Cbl added

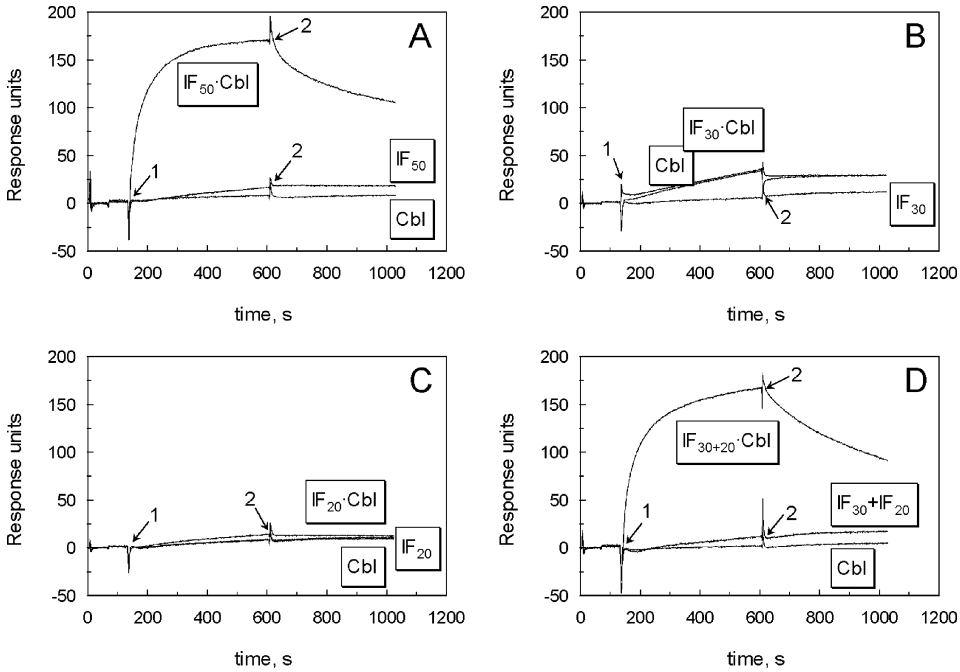

FIGURE 5: Interaction of IF variants with the receptor cubilin. IF, Cbl, or a mixture of each was exposed to a plasmon resonance chip coated with cubilin (*1*). The flow of the sample was changed to the buffer which caused dissociation of IF from the receptor (*2*). (A) Full-length IF_{50} (100 nM), Cbl (200 nM), or a mixture of each was exposed to cubilin. (B) N-Terminal fragment IF_{30} (100 nM), Cbl (50 μM), or a mixture of each was exposed to cubilin. (C) C-Terminal fragment IF_{20} (100 nM), Cbl (5 μM), or a mixture of each was exposed to cubilin. (D) Two fragments, IF_{30} and IF_{20} (100 and 200 nM, respectively), Cbl (200 nM), or a mixture of each was exposed to cubilin.

at high concentrations to saturate IF_{30}. The mixture of two peptides, IF_{30} and IF_{20}, was also incapable of receptor binding in the absence of Cbl. On the other hand, the IF_{30}/IF_{20} sample with added Cbl (Figure 5D) interacted with cubilin in a manner identical to that of IF_{50}·Cbl (Figure 5A).

DISCUSSION

In this paper, we investigate (i) the kinetics of Cbl binding to the specific protein IF, (ii) the assembly of the protein domains by the ligand, and (iii) the recognition of holo-IF by the receptor. The protein was purified from the recombinant plants by affinity chromatography (*6*, *13*) and devoid of Cbl by GdnHCl treatment. Three unsaturated apo forms (the full-length binder IF_{50}, the N-terminal peptide IF_{30}, and the C-terminal glycopeptide IF_{20}) were isolated as described previously (*13*). The renatured proteins induced the typical changes in the spectrum of Cbl upon its binding (Figure 1). They also demonstrated a high affinity for Cbl (Figure 4) and normal interaction with the receptor (Figure 5). The fraction of the active protein (AP) was determined by a new spectral method suggested in section 1 of the Appendix. The obtained value of AP (0.97 ± 0.03) indicated a high recovery of the protein.

We started our investigation from the partial reactions between the fragments and the ligand: IF_{30} + Cbl and IF_{20} + Cbl. Taken in these combinations, the reactants did not produce any oligomers (*13*) and obeyed the bimolecular reversible kinetics (section 2 of the Appendix and ref *20*). Experiments on the direct interaction between the peptides and Cbl (Figure 2A,B), as well as competition with a Cbl specific resin (Figure 3), revealed (i) the low affinity of IF_{30} for Cbl and (ii) a relatively good binding of IF_{20} to Cbl (Table 2), when compared with the K_{Cbl} of ≤ 1 pM determined for the full-length IF_{50} (Figure 4A,B, this publication and ref *11*). This finding was not anticipated, because the regions with a high degree of homology (*21*, *22*) and four of five potential Cbl binding sites (*23*) are located on the low-affinity fragment IF_{30}.

Although the binding of Cbl to pure IF_{30} was weak, this "inferior" peptide proved to be essential for retention of the ligand. Thus, rapid formation of the heterologous two-peptide complex, IF_{30+20}·Cbl, was detected in the IF_{30}+IF_{20}·Cbl mixture during the stopped-flow (Figure 2C) and light scattering experiments (*13*). Binding of the ligand by this complex was much stronger than by the isolated IF_{20}·Cbl complex, saying nothing about IF_{30}·Cbl. In fact, the ability of IF_{30} and IF_{20} to hold Cbl was quite comparable with the corresponding feature of the full-length protein IF_{50} judged from their dissociation rate constants (Figures 3A and 4D and Table 2). Firm encapsulation of Cbl inside the reassembled IF_{30+20}·Cbl construction indicated practically normal organization of its ligand site. Therefore, we came to a conclusion that interaction of Cbl with fragments IF_{30} and IF_{20} closely imitates binding to the native form, IF_{50}. In this regard, one might speculate that the protein sequence of IF_{20} comprises the primordial Cbl binding site, which was later built up and refined by attachment of the IF_{30} unit.

Investigation of the partial reactions made detailed reconstruction of the ligand binding in the IF_{30}/IF_{20}/Cbl mixture possible (see Figure 6A). This case seems to be relevant also in vivo because the associating fragments of gastric IF have been described in the literature (*24*). The presented minimal model ignores IF_{30}−Cbl, IF_{30}−IF_{30}, IF_{20}−IF_{20}, and IF_{30}−IF_{20} interactions as statistically insignificant (see Figures 2 and 3 and ref *13*). The assumptions outlined above reduced the complexity of the model and allowed us to draw a linear scheme with only two steps. First, Cbl binds to IF_{20} with the shown rate constants. At the next step, IF_{30} approaches IF_{20}·Cbl, and in most cases, two peptides build the ac-

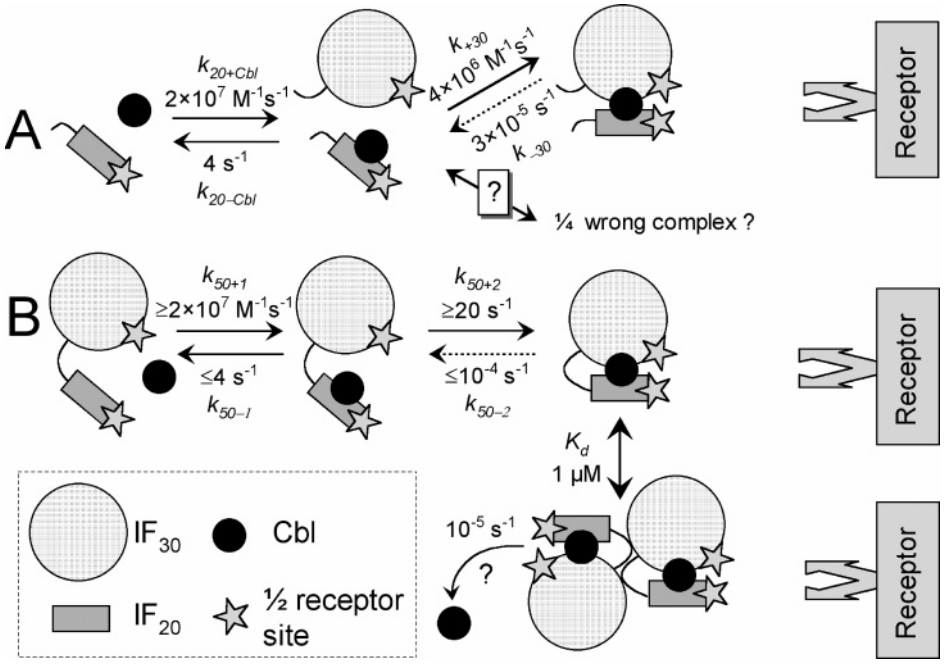

FIGURE 6: Binding of Cbl to IF and ligand-induced assembly of the domains (minimal schemes). (A) Interaction of Cbl with IF fragments. Cbl preferentially binds to IF_{20}, whereupon their complex interacts with IF_{30}. The produced monomer "glued" by Cbl reconstructs both the ligand binding site and the receptor recognition site. However, it cannot dimerize because of the damaged interdomain link. (B) Interaction of Cbl with full-length IF_{50}. Initial binding of Cbl to the C-terminal domain (IF_{20}) is followed by interaction with the N-terminal part (IF_{30}). Two connected domains encapsulate Cbl and form the receptor recognition site. In vitro dimerization is possible at high protein concentrations. See the text for the details.

complished ligand site (Figure 6A, top branch). As follows from the scheme, the disassembly of the IF_{30+20}·Cbl complex is limited by detachment of IF_{30} with the rate constant k_{-30}. The data on Cbl exchange (Figure 4D) allowed us to evaluate this constant since $k_{-app} = k_{-30}$.

Association of the fragments with the tight peptide−ligand complex was also possible at physiological protein concentrations ($[IF_{30}] = [IF_{20}] = 10-50$ nM) and ligand concentrations ([Cbl] = 2 nM) (Figure 4C). The binding kinetics for IF_{30} with IF_{20} and Cbl in Figure 4C was expected to be exponential according to the scheme in Figure 6A (top branch), yet two phases were discovered. We assume that the first phase reflects the appearance of the firm IF_{30+20}·Cbl complex assembled in the correct manner. At the same time, one can speculate about a parallel formation of a loose IF_{20}·Cbl··· IF_{30} aggregate as a consequence of erroneous collision between IF_{30} and IF_{20}·Cbl (Figure 6A, bottom branch). Such aggregates appear with a probability of ≈20% and are reassembled during tight fixation of the ligand either directly or via complete dissociation of the unproductive formation.

The IF_{30+20}·Cbl composite construction seemed to restore all the normal properties of the native protein; however, it could not dimerize (*13*). We explained this phenomenon by some damage in the corresponding site (*13*), as schematically shown in Figure 6A. The physiological role of IF dimerization remains unknown because the dimers are unstable and dissociate easily, at least under in vitro conditions.

Thorough examination of the partial reactions simplified analysis of the biphasic interaction between full-length IF_{50} and Cbl (Figure 2D). Thus, the first phase probably reflected the ligand binding to the C-terminal domain of IF_{50}. The second phase was attributed to assembly of the domains, where the detected rate constant may actually correspond to the last step in a series of transitions. Interaction between the domains seemed to be a quite sensitive affair, because expression of the second phase varied between IF_{50} preparations. The observed difference could be caused by slight changes during preparation of apo-IF which influenced coordination of the domains. This subject requires the following clarification. The final model of interaction between monomeric IF_{50} and Cbl included two steps and is shown in Figure 6B. The rate constants of the forward reactions were obtained directly from the experiments depicted in Figures 2D and 4A,B (10 min curves). As for the reverse reactions, we assumed k_{50-1} to be equal or less than k_{20-Cbl} of isolated IF_{20}. The rate coefficient for detachment of the IF_{30} domain (k_{50-2}) was calculated indirectly from the experiment at low protein concentrations where no dimerization was possible (Figure 4A,B, 22 h curves). Thus, the assumed equilibrium constant $K_{50,Cbl}$ of ≤1 pM was used to evaluate k_{50-2} according to the equation $K_{50,Cbl} = K_{50,1}/(1 + k_{50+2}/k_{50-2})$.

It is unclear to what extent dimerization of IF_{50}·Cbl with a K_d of 1 μM (*13*) influences dissociation of Cbl, yet, a "chase" experiment at a high concentration of IF (Figure 4D) allows us to make a prognosis. The process was simulated with the rate constants from Figure 6B considering equal parameters for H_2OCbl and CNCbl. The dashed curves in Figure 4D show the results of modeling, going from top to bottom: (1) IF_{30} and IF_{20}, (2) IF_{50} with prohibited dimerization or "leaking" dimer, and (3) IF_{50} with allowed dimerization ("dim") when the dimers do not liberate Cbl. The produced curves point to an insignificant effect of dimerization on Cbl retention. This indicates either the direct leakage of Cbl from the dimers or the existence of half-open dimers omitted in Figure 6B for the sake of simplicity.

The investigation demonstrates that interaction of Cbl with IF is a complex process. Formation of a composite binding

site with two domains "glued" together by Cbl requires the correct shape of the ligand. The presence of a "wrong" substrate is expected to cause erroneous distance between the approaching domains which will preclude their "clasp". This can be a reason for the extraordinary selectivity of IF for Cbl (*4*) combined with a high affinity for the ligand. In that regard, we have to discuss the conflicting values of K_{Cbl} observed for all Cbl specific binders (*9*−*12*). The appropriate explanation may come from the saturation experiments depicted in Figure 4. The curves (typically used for K_{Cbl} calculations) show that the insufficient incubation time of the protein−ligand mixture, as well as application of inappropriate equations, will result in severe overestimation of K_{Cbl}. It should be also stressed that the point of half-saturation for an E + S ↔ ES binding reaction does not correspond to $S_{1/2} = K_S$ but to $S_{1/2} = 0.5E_0 + K_S$ (where E_0 is the total concentration of the binding sites). These considerations may explain the K_{Cbl} values of ≥100 pM reported often in the literature.

The exceptional ligand selectivity is not the only particular feature of IF. Thus, only Cbl-saturated IF·Cbl is recognized by the receptor cubilin (*5*, *6*), whereas two other binders interact with their receptors in both apo and holo forms (*1*, *2*). Dissection of IF into two fragments provided an opportunity to test different IF domains, whether they carry the receptor recognition site. As one can see from panels B and C of Figure 5, none of the isolated fragments was capable of inducing a response from the cubilin-coated chip. The presence of a saturating amount of Cbl did not change this situation. The mixture of the disconnected peptides IF_{30} and IF_{20} did not interact with the receptor either (Figure 5D). Only when the fragments were assembled by Cbl in one complex, IF_{30+20}·Cbl, did they bind to the receptor (Figure 5D) in a manner indistinguishable from that of IF_{50}·Cbl. We hypothesize that the recognition site is composed of at least two distant components situated on IF_{30} and IF_{20} domains. Assembly of two fragments (domains) by Cbl brings the scattered components of the receptor recognition site together, which makes IF·Cbl compatible with cubilin (Figure 6). We cannot completely rule out a situation in which interaction of two domains induces an essential conformational change in only one part of the molecule, either IF_{30} or IF_{20}, which dramatically increases its affinity for the receptor, yet at present, there is no evidence that can support this mechanism.

Analysis of the IF + Cbl, IF + IF, and IF + cubilin reactions allowed us to suggest a plausible model of ligand binding and receptor recognition. Following assays concerning behavior of the Cbl analogues under analogous conditions may provide more detailed information about the mechanism of Cbl assimilation.

ACKNOWLEDGMENT

We acknowledge gratefully the excellent technical assistance of A. L. Christensen and C. Jacobsen.

APPENDIX

1. Measurement of the Active Protein via the Absorbance Ratio. The spectrum of a Cbl-saturated binder is defined by two main components: the absorbance peak of the protein moiety (280 nm) and the γ-peak of Cbl (354 nm for H_2-OCbl and IF). The absorbance ratio R (A_{280}/A_{354}) of IF·Cbl can be expressed as follows:

$$R = \frac{(\epsilon_0^{280} + \mathrm{AP} \times \Delta\epsilon^{280})[\mathrm{IF}]}{(\epsilon_0^{354} + \mathrm{AP} \times \Delta\epsilon^{354})[\mathrm{IF}]} \tag{1.1}$$

where AP is the active protein presented as the fraction of total IF (AP = 0−1), ϵ_0^{280} and ϵ_0^{354} are the coefficients of molar absorbance for apo-IF, $\Delta\epsilon^{280}$ and $\Delta\epsilon^{354}$ are increments to ϵ_0 upon saturation with Cbl, and [IF] is the molar concentration of the binding sites. AP can be expressed via the known coefficients ϵ_0 and $\Delta\epsilon$ (Table 1) and the measured value of R:

$$\mathrm{AP} = \frac{\epsilon_0^{280} - R\epsilon_0^{354}}{R\Delta\epsilon^{354} - \Delta\epsilon^{280}} \tag{1.2}$$

2. Equations of Bimolecular Kinetics. A simple binding scheme can be written as

$$\mathrm{E} + \mathrm{S} \underset{k_{-s}}{\overset{k_{+s}}{\rightleftharpoons}} \mathrm{ES}$$

When the initial concentrations E_0 and S_0 are comparable, ES_{eq} at equilibrium is expressed via the function (*20*, *25*):

$$\mathrm{ES}_{eq} = \frac{E_0 + S_0 + K_s - \sqrt{(E_0 + S_0 + K_s)^2 - 4E_0S_0}}{2} \tag{2.1}$$

The dependence of ES_{eq} on S_0 can be used for calculation of both E_0 and K_s ($=k_{-s}/k_{+s}$) by either nonlinear regression analysis or a graphical method suggested by Dixon (*25*).

The time-dependent increase in the ES concentration from 0 to ES_{eq} (*20*) can be expressed as:

$$\mathrm{ES} = \mathrm{ES}_{eq}\left[1 - \frac{e^{-\sum kt}}{1 + \frac{k_{+s}\mathrm{ES}_{eq}}{\sum k}(1 - e^{-\sum kt})}\right] \tag{2.2}$$

where ES_{eq} is calculated via eq 2.1, t is time, and $\sum k$ is described by the equation

$$\sum k = k_{+s}(E_0 + S_0 - 2\mathrm{ES}_{eq}) + k_{-s} \tag{2.3}$$

Optionally, a response coefficient ϵ_Δ can be introduced into eqs 2.1 and 2.2 to relate absorbance A to concentration ES via $A = \epsilon_\Delta \mathrm{ES}$. The experimental points A versus t were subjected to the nonlinear regression analysis with two unknown regression parameters k_{+s} and k_{-s}.

The time dependence of an irreversible reaction ($k_{-s} = 0$) can be presented as

$$\mathrm{ES} = E_0\frac{1 - e^{-k_{+s}(S_0 - E_0)t}}{1 - \frac{E_0}{S_0}e^{-k_{+s}(S_0 - E_0)t}} \tag{2.4}$$

where k_{+s} is set as the regression parameter for the dependency $A = \epsilon_\Delta \mathrm{ES}$ versus t.

3. Two-Step Binding Model. The data are presented in Figure 2D. The curves were simulated using Gepasi 3.2 (*18*),

which calculates transient concentrations of all intermediates according to the kinetic scheme, the values of rate constants, and the initial concentrations of metabolites. The following scheme was employed:

$$E + S \xrightarrow{k_{+1}} E\cdots S \xrightarrow{k_{+2}} ES$$

where E and S are IF_{50} and Cbl, respectively. The appearance of E···S and ES was monitored over time, whereupon the optimal values of k_{+1} and k_{+2} were calculated by the regression analysis (*18*).

4. Stability of the Peptide−Cbl Complexes. The affinity of peptide E for ligand S was measured via a "competition" or "trap" experiment with a specific adsorbent (Figure 3). The initial velocity of S adsorption (v_{ads}) was measured at different E_0 concentrations. The scheme of interaction could be drawn as follows:

$$\begin{array}{ccc} & (fast) & \\ & K_s & \\ S + E & \leftrightarrows & ES \\ (slow)\downarrow k^{s}_{+a} & & \downarrow k^{es}_{-a}\ (very\ slow) \\ S\cdot A & & ES\cdot A \end{array}$$

where E, S, and A stand for peptide IF_{30} or IF_{20}, Cbl, and adsorbent, respectively, K_s is the dissociation constant of the fast equilibration between E and S, and $k_{+a}{}^{s}$ and $k_{+a}{}^{es}$ are the rate constant of S and ES adsorption, respectively. We did not indicate dissociation from the adsorbent because this process is irrelevant for analysis of the initial velocity of adsorption v_{ads}. The concentration of *A* was sufficiently high to be considered as a constant throughout the experiment. The dependency of v_{ads} on E_0 can be expressed as follows:

$$v_{ads} = k_{+a}{}^{s}A(S_0 - ES) + k_{+a}{}^{es}AES = k_{+a}{}^{s}AS_0 - k_{+a}{}^{s}AS_0\frac{ES}{S_0} + k_{+a}{}^{es}AS_0\frac{ES}{S_0}$$

where S_0 and E_0 are the total concentrations of the ligand and peptide, respectively, and ES is expressed in eq 2.1. Then, after separation of the constants, (i) $v_s = k_{+a}{}^{s}AS_0$ and (ii) $v_{es} = k_{+a}{}^{es}AS_0$, the above equation can be rewritten and used for calculation of K_s:

$$v_{ads} = v_s - (v_s - v_{es})\frac{ES}{S_0} \qquad (4)$$

The notation in eq 4 should be interpreted as follows. v_s and v_{es} are the initial velocities of S adsorption when $E_0 = 0$ and $E_0 \rightarrow \infty$, respectively (note that $S_0 = ES$ at $E_0 \rightarrow \infty$ in the equation for v_{es}). Fitting of the experimental data was performed using eq 4 with three regression coefficients: v_s, v_{es}, and K_s.

REFERENCES

1. Nexø, E. (1998) Cobalamin binding proteins, in *Vitamin B_{12} and B_{12}-Proteins* (Kräutler, B., Arigoni, D., and Golding, T., Eds.) pp 461−475, Wiley-VCH, Weinheim, Germany.
2. Moestrup, S. K., and Verroust, P. J. (2001) Megalin- and cubilin-mediated endocytosis of protein-bound vitamins, lipids, and hormones in polarized epithelia, *Annu. Rev. Nutr. 21*, 407−428.
3. Seetharam, B. (1999) Receptor mediated endocytosis of cobalamin (vitamin B_{12}), *Annu. Rev. Nutr. 19*, 173−195.
4. Stupperich, E., and Nexø, E. (1991) Effect of the cobalt-N coordination on the cobamide recognition by the human vitamin B12 binding proteins intrinsic factor, transcobalamin and haptocorrin, *Eur. J. Biochem. 199*, 299−303.
5. Birn, H., Verroust, P. J., Nexø, E., Hager, H., Jacobsen, C., Christensen, E. I., and Moestyrup, S. K. (1997) Characterization of an epithelial ≈460 kDa protein that facilitates endocytosis of intrinsic factor-vitamin B_{12} and binds receptor associated protein, *J. Biol. Chem. 272*, 26497−26504.
6. Fedosov, S. N., Laursen, N. B., Nexø, E., Moestrup, S. K., Petersen, T. E., Erik, Ø., Jensen, E. Ø., and Berglund, L. (2003) Human intrinsic factor expressed in the plant *Arabidopsis thaliana*, *Eur. J. Biochem. 270*, 3362−3367.
7. Ulleland, M., Eilertsen, I., Quadros, E. V., Rothenberg, S. P., Fedosov, S. N., Sundrehagen, E., and Ørning, L. (2002) Direct assay for cobalamin bound to transcobalamin (holo-transcobalamin) in serum, *Clin. Chem. 48*, 526−532.
8. Nexø, E., Hvas, A. M., Bleie, Ø., Refsum, H., Fedosov, S. N., Vollset, S. E., Schneede, J., Nordrehaug, J. E., Ueland, P. G., and Nygard, O. K. (2002) Holo-transcobalamin is an early marker of changes in cobalamin homeostasis. A randomized placebo-controlled study, *Clin. Chem. 48*, 1768−1771.
9. Marchaj, A., Jacobsen, D. W., Savon, S. R., and Brown, K. L. (1995) KInetics and thermodynamics of the interaction of cyanocobalamin (vitamin B_{12}) with haptocorrin: Measurement of the highest protein−ligand binding constant yet reported, *J. Am. Chem. Soc. 117*, 11640−11646.
10. Brada, N., Gordon, M. M., Wen, J., and Alpers, D. H. (2001) Transfer of cobalamin from intrinsic factor to transcobalamin II, *J. Nutr. Biochem. 12*, 200−206.
11. Fedosov, S. N., Berglund, L., Fedosova, N. U., Nexø, E., and Petersen, T. E. (2002) Comparative analysis of cobalamin binding kinetics and ligand protection for intrinsic factor, transcobalamin, and haptocorrin, *J. Biol. Chem. 274*, 26015−26020.
12. Cannon, M. J., Myszka, D. G., Bagnato, J. D., Alpers, D. H., West, F. G., and Grissom, C. B. (2002) Equilibrium and kinetic analysis of the interactions between vitamin B_{12} binding proteins and cobalamins by surface plasmon resonance, *Anal. Biochem. 305*, 1−9.
13. Fedosov, S. N., Fedosova, N. U., Berglund, L., Moestrup, S. K., Nexø, E., and Petersen, T. E. (2004) Assembly of the intrinsic factor domains and oligomerization of the protein in the presence of cobalamin, *Biochemistry 43*, 15095−15102.
14. Nexø, E. (1975) A new principle in biospecific affinity chromatography used for purification of cobalamin-binding proteins, *Biochim. Biophys. Acta 379*, 189−192.
15. Pace, C. N., Vajdos, F., Fee, L., Grimsley, G., and Gray, T. (1995) How to measure and predict the molar absorption coefficient of a protein, *Protein Sci. 4*, 2411−2423.
16. Fedosov, S. N., Fedosova, N. U., Nexø, E., and Petersen, T. E. (2000) Conformational changes of transcobalamin induced by aquocobalamin binding. Mechanism of substitution of the cobalt-coordinated group in the bound ligand, *J. Biol. Chem. 275*, 11791−11798.
17. Lau, K. S., Gottlieb, C., Wasserman, L. R., and Herbert, W. (1965) Measurement of serum B_{12} level using radioisotope dilution and coated charcoal, *Blood 26*, 202−214.
18. Mendes, P. (1997) Biochemistry by numbers: Simulation of biochemical pathways with Gepasi 3, *Trends Biochem. Sci. 22*, 361−363.
19. Nexø, E., and Olesen, H. (1976) Changes in the ultraviolet and circular dichroism spectra of aquo-, hydroxy-, azido-, and cyanocobalamin when bound to human intrinsic factor or human transcobalamin I, *Biochim. Biophys. Acta 446*, 143−150.
20. Andraos, J. (1999) A streaming approach to solving simple and complex kinetic systems automatically, *J. Chem. Educ. 76*, 1578−1583.
21. Li, N., Seetharam, S., Lindemans, J., Alpers, D. H., Arwert, F., and Seetharam, B. (1993) Isolation and sequence analysis of variant forms of human transcobalamin II, *Biochim. Biophys. Acta 1172*, 21−30.
22. Fedosov, S. N., Berglund, L., Nexø, E., and Petersen, T. E. (1999) Sequence, S−S bridges, and spectra of bovine transcobalamin expressed in *Pichia pastoris*, *J. Biol. Chem. 274*, 26015−26020.
23. Wen, J., Kinnear, M. B., Richardson, M. A., Willetts, N. S., Russel-Jones, G. J., Gordon, M. M., and Alpers, D. H. (2000) Functional expression in *Pichia pastoris* of human and rat intrinsic factor, *Biochim. Boiphys. Acta 1490*, 43−53.

24. Christensen, J. M., Hippe, E., Olesen, H., Rye, M., Haber, E., Lee, L., and Thomsen, J. (1973) Purification of human intrinsic factor by affinity chromatography, *Biochim. Biophys. Acta 303*, 319−332.

25. Dixon, M., and Webb, E. C. (1972) The graphical determination of K_m and K_i, *Biochem. J. 1*, 197−202.

BI047936V